EFFECT OF STREAMWISE AND PREFERENTIAL DIFFUSION ON CYLINDRICAL BURKE-SCHUMANN FLAMES

S.R. Lee* and S.H. Chung*

(Received January 23, 1991)

Effect of streamwise and preferential diffusion on cylindrical Burke-Schumann flame has been analyzed using perturbation method and Green's function technique. Results show that for large Peclet number, streamwise diffusion has little effect, while for small Pe, it is balanced with radial diffusion such that a finite minimum flame height exists. Preferential diffusion induces flame temperature variation along the flame surface and the results agree qualitatively with existing experimental data. It also shows that the symmetry in flame temperature variation by the sign of (Le-1) in two dimensional case does not hold in cylindrical flames due to focusing and defocusing effects of mass and thermal diffusion by the radial curvature of flame.

Key Words :Burke-Schumann Flame, Flame Temperature, Preferential Diffusion

NOMENCLATURE

a : Radius of inner nozzle
b : Radius of outer cylinder
c : a/b
C_p : Specific heat
D_i : Mass diffusivity of i-th species
$g_n(z|z_o)$: Element of Green's function
$G(r|r_o)$: Green's function
h_j : Defined in Eq.(A2)
H_j : Defined in Eq.(18)
k : Pe/2
l_i : $1\text{-}1/Le_i$
Le_i : Lewis number of i-th species $(\lambda/(\rho D_i C_p))$
$\boldsymbol{n}$: Unit normal vector
Pe : Peclet number $(=\rho v b/(\lambda/C_p))$
Q : Heat of combustion per unit mass of fuel
r : Radial coordinate
$\boldsymbol{r}$: Coordinate vector
$\boldsymbol{r}_o$: Coordinate vector of the source
R_T : Radius of curvature at flame tip
S : Surface
U_n : Function defined in Eq.(20)
V : Volume
v : Velocity
Y_i : Mass fraction of species i
z : Streamwise coordinate
Z_f : Flame height in the leading order

Greek Symbols

α_n : $(Pe^2+\lambda_n)^{1/2}$
β_j : Coupling function
Γ : Function defined in Eq.(22)
δ_n : Function defined Eq.(A41)
$\delta(\boldsymbol{r}-\boldsymbol{r}_o)$: Dirac delta function
θ_j : Function defined in Eq.(A1)
λ : Thermal conductivity
λ_n : Eigen value
ν : $(Y_{oo}/\sigma Le_O)/(Y_{Fo}/Le_F)$
ρ : Density
σ : Stoichiometric oxidizer to fuel mass ratio
ϕ_n : Function defined in Eq.(A31)

Superscripts

0 : Leading order
1 : First order
~ : Stoichiometrically adjusted quantity
* : State with $Le_i=1$

Superscripts

D : Dirichlet boundary
F : Fuel
i : i-th species
N : Neumann boundary
O : Oxidizer
S : Species
T : Temperature
o : Nozzle exit or source

*Department of Mechancial Engineering, Seoul National University, Seoul 151-742, Korea

1. INTRODUCTION

The Burke-Schumann (B-S) flame has been widely adopted in studying diffusion flame characteristics because of its convenience in analysis and in setting up experiment in a laboratory. Burke and Schumann(1928) has predicted the flame shapes through the analysis of species conservation equations in the coupling function formulation assuming unity Lewis numbers and balance of streamwise convection and transverse diffusion. It can be easily shown that the flame temperature is uniform and is equal to the adiabatic one (Williams, 1985).

Transverse diffusion in B-S system can be neglected on the basis of the existence of the outer tube and the axis of symmetry. However, the streamwise diffusion can only be neglected when the streamwise convection is large, that is,

for large Peclet number Pe. Recent interests in the B-S flames with relation to the modeling of composite rocket propellants (Cohen, 1980) indicate that the streamwise diffusion should be accounted for, since typical length scale is the order of 100 μ such that the Peclet number is expected to be small.

Preferential diffusion due to the difference in intensities between mass and thermal diffusions, which can be characterized by Lewis number Le, is considered to be an important factor affecting flame propagation, stability and extinction for premixed flames (Sivashinsky, 1983; Buckmaster and Ludford, 1982; Chung and Law, 1989; Law et al., 1982).

Effect of preferential diffusion on diffusion flames has also been analyzed (Law and Chung, 1982; Chung and Law, 1983) which affects flame temperature and thereby extinction. It can be reasoned that such phenomena as tip opening, partial blowoff, and sooting height (Glassman and Yaccarino, 1981) in diffusion flame can be explained on the basis of preferential diffusion.

Accounting these effects of streamwise and preferential diffusions, Chung and Law(1984) analyzed the two-dimensional B-S flame showing that the flame temperature varies spatially depending on $(Le\text{-}1)$ and Pe. However, the practical B-S flame is the cylindrical one where the focusing and defocusing effects of mass and thermal diffusions would demonstrate different characteristics compared to the two-dimensional one.

Thus the objective of the present study is to analyze the effects of streamwise and preferential diffusions in the cylindrical B-S flame.

2. GOVERNING EQUATIONS

Governing equations with streamwise and preferential diffusions in the cylindrical coordinates are(Burke and Schumann, 1928; Williams, 1988)

$$Pe\frac{\partial(\tilde{Y}_F+\tilde{T})}{\partial z}-\frac{1}{Le_F}\left\{\frac{1}{r}\frac{\partial}{\partial r}\left(r\frac{\partial\tilde{Y}_F}{\partial r}\right)+\frac{\partial^2\tilde{Y}_F}{\partial z^2}\right\}-\left\{\frac{1}{r}\frac{\partial}{\partial r}\left(r\frac{\partial\tilde{T}}{\partial r}\right)+\frac{\partial^2\tilde{T}}{\partial z^2}\right\}=0 \tag{1}$$

$$Pe\frac{\partial(\tilde{Y}_F-\tilde{Y}_O)}{\partial z}-\frac{1}{Le_F}\left\{\frac{1}{r}\frac{\partial}{\partial r}\left(r\frac{\partial\tilde{Y}_F}{\partial r}\right)+\frac{\partial^2\tilde{Y}_F}{\partial z^2}\right\}+\frac{1}{Le_O}\left\{\frac{1}{r}\frac{\partial}{\partial r}\left(r\frac{\partial\tilde{Y}_O}{\partial r}\right)+\frac{\partial^2\tilde{Y}_O}{\partial z^2}\right\}=0 \tag{2}$$

where r and z are the radial and streamwise coordinates, respectively, nondimensionalized with the outer tube radius b, $\tilde{T}=C_pT/QY_{Fo}$, $\tilde{Y}_F=Y_F/Y_{Fo}$, $\tilde{Y}_O=Y_O/\sigma Y_{Fo}$, T the temperature, Y the mass fraction, Q the heat of combustion per unit mass of fuel, σ the stoichiometric oxidizer to fuel mass ratio, subscripts F, O, and o the fuel, oxidizer, and condition at the nozzle exit, respectively, $Le_i=\lambda/(\rho C_pD_i)$ and $Pe=\rho vb/(\lambda/C_p)$. Here ρ is the density, v the streamwise velocity, C_p, λ, and D_i the specific heat, thermal conductivity, and mass diffusivity, respectively, which are assumed constants. To suppress the effect of shear layer mixing near nozzle exit, ρv is assumed uniform.

Boundary conditions are

$$\begin{aligned}
&0<r<c,\ z=0 \quad ;\ \tilde{Y}_F=1,\ \tilde{T}=\tilde{T}_o\\
&c<r<1,\ z=0 \quad ;\ \tilde{Y}_O=\tilde{Y}_{Oo},\ \tilde{T}=\tilde{T}_o\\
&0<r<1,\ z\to\infty\ ;\ \text{bounded}\\
&r=0,\ z>0 \quad ;\ \partial(.)/\partial r=0\ (\text{axisymmetric})\\
&r=1,\ z>0 \quad ;\ \partial(.)/\partial r=0\ (\text{adiabatic and impermeable})
\end{aligned} \tag{3}$$

where $c=a/b$ and a the fuel nozzle radius.

3. ANALYSIS

Similar to the two dimensional case, Eqs.(1) and (2) exhibit exact solutions for several special cases and these cases will be considered first.

3.1 Special Cases

When the Lewis numbers are all unity, Eqs.(1) and (2) have the following Shvab-Zeldovich coupling functions

$$Pe\frac{\partial\beta_j^*}{\partial z}-\left\{\frac{1}{r}\frac{\partial}{\partial r}\left(r\frac{\partial\beta_j}{\partial r}\right)+\frac{\partial^2\beta_j}{\partial z^2}\right\}=0,\ j=S,\ T \tag{4}$$

where $\beta_S=\tilde{Y}_F/Le_F-\tilde{Y}_O/Le_O$ and $\beta_T=\tilde{Y}_F/Le_F+\tilde{T}$. Superscript* indicates the case with unity Lewis numbers such that $\beta_S^*=\tilde{Y}_F-\tilde{Y}_O$ and $\beta_T^*=\tilde{Y}_F+\tilde{T}$.

For large Pe, characteristic z scale becomes large, hence the streamwise convection is much larger than the streamwise diffusion. Thus Eq.(4) becomes identical to that of the original B-S formulation(1928). For small Pe, however, the streamwise diffusion can be stronger than the streamwise convection such that the original B-S solution is expected to break down.

Using separation of variables, the solution of Eq.(4) becomes

$$\beta_S^*=\{c^2(1+\tilde{Y}_{Oo})-\tilde{Y}_{Oo}\}+2c(1+\tilde{Y}_{Oo})\sum_{n=1}^{\infty}\frac{J_1(\lambda_nc)}{\lambda_nJ_0^2(\lambda_n)}J_o(\lambda_nr)\exp\left(\frac{Pe-\alpha_n}{2}z\right) \tag{5}$$

$$\beta_T^*=(c^2+\tilde{T}_o)+2c\sum_{n=1}^{\infty}\frac{J_1(\lambda_nc)}{\lambda_nJ_0^2(\lambda_n)}J_0(\lambda_nr)\exp\left(\frac{Pe-\alpha_n}{2}z\right) \tag{6}$$

where $\alpha_n=(Pe^2+4\lambda_n^2)^{1/2}$. Eqs.(5) and (6) show that the Pe influences α_n only. As $Pe\to\infty$, $(Pe-\alpha_n)\to-2\lambda_n^2/Pe$ and the solution approaches the original B-S solution. However, as $Pe\to0$, $(Pe-\alpha_n)\to-2\lambda_n$ and this is independent of Pe. Thus, the original B-S solution can not be applied to the small Pe limit.

In the flame sheet limit, the fuel and oxidizer are completely consumed and the flame location can be determined from Eq.(5) by setting $\beta_S^*=0$. These results are compared with the original B-S solution in Fig. 1 for over-($\tilde{Y}_{Oo}=0.4$) and under-ventilated($\tilde{Y}_{Oo}=0.2$) cases with $c=0.5$. This shows that the flame height was underpredicted by neglecting the streamwise diffusion. Especially for $Pe=0$, there exists a finite length of the flame height while it is zero if the streamwise diffusion is neglected shown in Fig. 2.

For nonunity Le_i, Shvab-Zeldovich coupling function does not exist in general. However, there are two cases in which the coupling function formulation is possible. One is the case with $Pe=0$ and the other with $Le_F=Le_O$. These can be used to test the accuracy of the general Lewis number problem.

For $Pe=0$ Eqs.(1) and (2) becomes

$$\frac{1}{r}\frac{\partial}{\partial r}\left(r\frac{\partial\beta_j}{\partial r}\right)+\frac{\partial^2\beta_j}{\partial z^2}=0,\qquad j=S,\ T \tag{7}$$

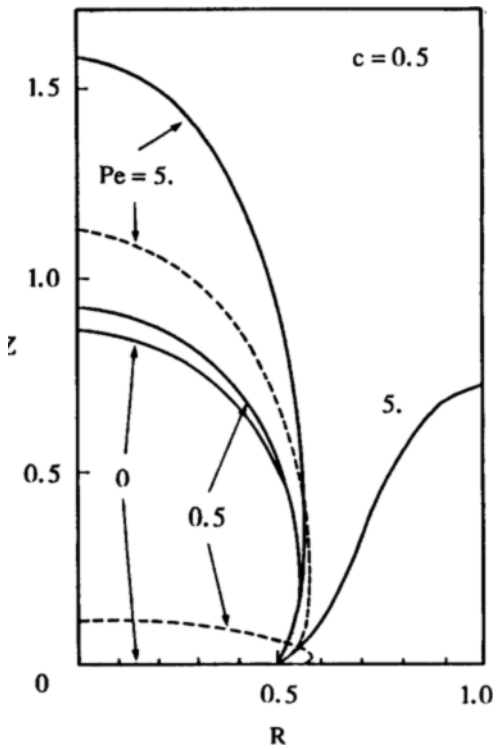

Fig. 1 Comparison of flame shapes for over-($\tilde{Y}_{Oo}=0.4$) and under-ventilated($\tilde{Y}_{Oo}=0.2$) cases(—— : present solution, ···; original B-S solution)

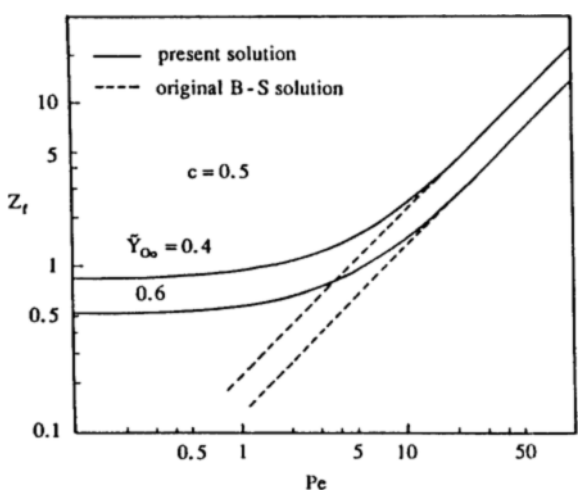

Fig. 2 Flame heights as function of Pe

and the solution can be found as folows.

$$\beta_S=\left\{c^2\left(\frac{1}{Le_F}+\frac{\tilde{Y}_{Oo}}{Le_O}\right)-\frac{\tilde{Y}_{Oo}}{Le_O}\right\}+2c\left(\frac{1}{Le_F}+\frac{\tilde{Y}_{Oo}}{Le_O}\right)\sum_{n=1}^{\infty}\frac{J_1(\lambda_n c)}{\lambda_n J_0^2(\lambda_n)}J_0(\lambda_n r)\exp(-\lambda_n z) \tag{8}$$

$$\beta_T=\left(\frac{c^2}{Le_F}+\tilde{T}_O\right)+\frac{2c}{Le_F}\sum_{n=1}^{\infty}\frac{J_1(\lambda_n c)}{\lambda_n J_0^2(\lambda_n)}J_0(\lambda_n r)\exp(-\lambda_n z) \tag{9}$$

The flame location(r_f, z_f), determined from $\beta_S=0$ becomes

$$\{c^2(1+\nu)-\nu\}+2c(1+\nu)\sum_{n=1}^{\infty}\frac{J_1(\lambda_n c)}{\lambda_n J_0^2(\lambda_n)}J_0(\lambda_n r_f)\exp(-\lambda_n z_f)=0 \tag{10}$$

which is functions of c and $\nu=Y_{Oo}/\sigma Le_O)/(Y_{FO}/Le_F)$ only. If we consider the effect of Lewis number by defining effective mass fraction $Y_{i,eff}=Y_i/Le_i$, then this solution is identical to the original B-S one using $Y_{i,eff}$ instead of Y_i for the case of $Le_i=1$. If Le_F/Le_O increases, then it has the same effect of increasing Y_{Oo} or decreasing Y_{FO} from the definition of ν. Hence, it is easily conceivable that the flame height will be shortened for an overventilated flame while lengthened for underventilated one.

Flame temperature can be found from Eqs.(8) and (10) as follows.

$$\frac{C_p(T_f-T_O)}{Y_{Oo}/\sigma Le_O)}+\frac{C_p(T_f-T_O)}{(Y_{FO}/Le_F)}=Q \tag{11}$$

This indicates that the increase in Le_i has the same effect of decreasing the boundary concentrations of reactants. Hence the flame temperature becomes higher(lower) than the adiabatic one as the Lewis number decreases (increases) from unity.

Another type of special case is for $Le_F=Le_O=Le$. In such a case there exists a coupling function for species as follows.

$$PeLe\frac{\partial\beta_S^*}{\partial z}-\left\{\frac{1}{r}\frac{\partial}{\partial r}\left(r\frac{\partial\beta_S^*}{\partial r}\right)+\frac{\partial^2\beta_S^*}{\partial z^2}\right\}=0 \tag{12}$$

By defining $Pe_{eff}=Pe\ Le$, this becomes identical to the case using Pe_{eff} instead of using Pe for $Le=1$. Since the flame height increases with Pe for $Le=1$, it will increase by increasing Le for the present case. Coupling function for temperature, however, does not exist in this case.

3.2 General Case ($Le_i\cong 1$)

The solution of the elliptic partial differential equations for general Lewis numbers is sought assuming small($1\text{-}1/Le_i$) and using it as a small parameter in perturbation analysis.

Jump conditions at the flame sheet for general Lewis numbers are as follows(Chung and Law, 1983).

$$\{\boldsymbol{n}\cdot\nabla(\tilde{Y}_F/Le_F)\}^{r_f-}=\{\boldsymbol{n}\cdot\nabla(\tilde{Y}_O/Le_O)\}^{r_f-}$$
$$[\boldsymbol{n}\cdot\nabla\tilde{T}]^{r_f-}=\{\boldsymbol{n}\cdot\nabla(\tilde{Y}_F/Le_F)\}^{r_f-} \tag{13}$$

Since heat and reactant mass can not be accumulated at a sheet, it can be readily seen that the coupling functions should be chosen as $\beta_S=\tilde{Y}_F/Le_F-\tilde{Y}_O/Le_O$, $\beta_T=\tilde{Y}_F/Le_F+\tilde{T}$ to satisfy Eq.(13) in all orders.

Equations(1) and (2) can be rearranged as follows.

$$Pe\frac{\partial\beta_T}{\partial z}-\left\{\frac{1}{r}\frac{\partial}{\partial r}\left(r\frac{\partial\beta_T}{\partial r}\right)+\frac{\partial^2\beta_T}{\partial z^2}\right\}=Pe\left(\frac{1}{Le_F}-1\right)\frac{\partial\tilde{Y}_F}{\partial z} \tag{14}$$

$$Pe\frac{\partial\beta_S}{\partial z}-\left\{\frac{1}{r}\frac{\partial}{\partial r}\left(r\frac{\partial\beta_S}{\partial r}\right)+\frac{\partial^2\beta_S}{\partial z^2}\right\}=Pe\left(\frac{1}{Le_F}-1\right)\frac{\partial\tilde{Y}_F}{\partial z}+Pe\left(\frac{1}{Le_O}-1\right)\frac{\partial\tilde{Y}_O}{\partial z} \tag{15}$$

By dfining $1_i=(1-1/Le_i)$ and using 1_F as a small parameter, $\tilde{T}$ and $\tilde{Y}_i$ can be expanded as follows.

$$\tilde{T}=\tilde{T}^0+1_F\tilde{T}^1+\cdots$$
$$\tilde{Y}_i=\tilde{Y}_i^0+1_F\tilde{Y}_i^1+\cdots \tag{16}$$

Substituting into Eqs. (14) and (15) and rearranging terms of same order

$$1_F^0 : Pe\frac{\partial\beta_j^0}{\partial z}-\left\{\frac{1}{r}\frac{\partial}{\partial r}\left(r\frac{\partial\beta_j^0}{\partial r}\right)+\frac{\partial^2 B_j^0}{\partial z^2}\right\}=0 \tag{17}$$

$$1_F^1 : Pe\frac{\partial\beta_j^1}{\partial z}-\left(\frac{1}{r}\frac{\partial}{\partial r}\left(r\frac{\partial\beta_j^1}{\partial r}\right)+\frac{\partial^2\beta_j^1}{\partial r}\right)+\frac{\partial^2\beta_j^1}{\partial z^2}\Big\}=H_j,\quad j=T,S \tag{18}$$

where $\beta_T^k=\tilde{T}^k-\tilde{Y}_F^k/Le_F$, $\beta_S^k=\tilde{Y}_F^k/Le_F-\tilde{Y}_O^k/Le_O$, $H_T=-Pe\partial\tilde{Y}_F^0/\partial z$ and $H_S=-Pe\partial\{\tilde{Y}_F^0-(1_O/1_F)\tilde{Y}_O^0\}/\partial z$. Since Eq. (17) should satisfy the boundary conditions, Eq. (18) should have homogeneous boundary conditions.

Separation of variables can be used to find the solution of Eq. (17), however, the solution of Eq. (18) can not be found. Thus, Green's function technique has been adopted to find the solution (ref. Appendix).

4. RESULTS AND DISCUSSIONS

The solutions of Eqs. (17) and (18) are

$$\beta_T^0=\left(\frac{c^2}{Le_F}+\tilde{T}_O\right)+\frac{2c}{Le_F}\sum_{n=1}^{\infty}\frac{J_1(\lambda_n c)}{\lambda_n J_0^2(\lambda_n)}J_0(\lambda_n r)\exp\left(\frac{Pe-\alpha_n}{2}z\right) \tag{19}$$

$$\beta_S^0=\left\{c^2\left(\frac{1}{Le_F}+\frac{\tilde{Y}_{OO}}{Le_O}\right)-\frac{\tilde{Y}_{OO}}{Le_O}\right\}+2c\left(\frac{1}{Le_F}+\frac{\tilde{Y}_{OO}}{Le_O}\right)\sum_{n=1}^{\infty}\frac{J_1(\lambda_n c)}{\lambda_n J_0^2(\lambda_n)}J_0(\lambda_n r)\exp\left(\frac{Pe-\alpha_n}{2}z\right) \tag{20}$$

$$\beta_S^1=\left(1-\frac{Le_O-1}{Le_F-1}\right)\beta_T^1-\frac{Le_O-1}{Le_F-1}Pez\sum_{n=1}^{\infty}\phi_n J_0(\lambda_n r)\exp\left(\frac{Pe-\alpha_n}{2}z\right)/\alpha_n \tag{21}$$

with β_T^1 for
overventilated case;

$$\beta_T^1=-2Pe\exp\left(\frac{Pe}{2}z\right)\left[\sum_{m=1}^{\infty}\int_0^{z_f}\phi_m U_O\exp\left(-\frac{\alpha_m}{2}z_O\right)\frac{r_f^O J_1(\lambda_m r_f^O)}{\lambda_m}dz_O+\sum_{n=1}^{\infty}\frac{J_0(\lambda_n r)}{J_0^2(\lambda_n)}\int_0^{z_f}U_n\phi_n\exp\left(-\frac{\alpha_n}{2}z_O\right)\frac{r_f^{O2}}{2}\{J_1^2(\lambda_n r_f^O)+J_0^2(\lambda_n r_f^O)\}dz_O+\sum_{n=1}^{\infty}\frac{J_0(\lambda_n r)}{J_0^2(\lambda_n)}\int_0^{z_f}U_n\sum_{\substack{m=1\\ m\neq n}}^{\infty}\phi_m\exp\left(\frac{\alpha_m}{2}z_O\right)\frac{r_f^{O2}}{\lambda_m^2-\lambda_n^2}\times\{\lambda_m J_0(\lambda_n r_f^O)J_1(\lambda_m r_f^O)-\lambda_n J_0(\lambda_m r_f^O)J_1(\lambda_n r_f^O)\}dz_O\right]\equiv\Gamma \tag{22}$$

underventilated case;

$$\beta_T^1=\Gamma-Pe\exp\left(\frac{Pe}{2}z\right)\sum_{n=1}^{\infty}J_0(\lambda_n r)\,\delta_n/2 \tag{23}$$

Here, the zeroth order solutions β_S^0 are identical to that derived using separation of variables.

The flame sheet location and temperature up to the first order in 1_F can be determined from $\beta_S^0+1_F\beta_S^1=0$ and $\tilde{T}_f=\tilde{T}^0(r_f^1, z_f^1)+1_F\tilde{T}^1(r_f^1, z_f^1)=\beta_T^0(r_f^1, z_f^1)+1_F\beta_T^1(r_f^1, z_f^1)$. This perturbation solution with equal Lewis numbers for fuel and oxidizer, compared to the exact solution of Eq. (12), has the same accuracy as the one in Chung and Law (1984) for $|Le_i-1|\leq 0.3$.

Change in flame shape by Lewis number variations is shown in Fig. 3 for small Peclet number of $Pe=5$. For this over-ventilated case, flame becomes larger as Le_F decreases

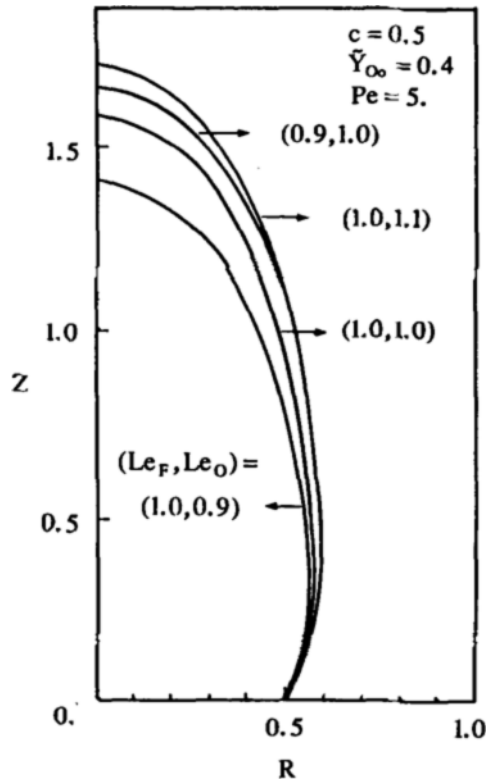

Fig. 3 Effect of Lewis numbers on flame shape for small Pe

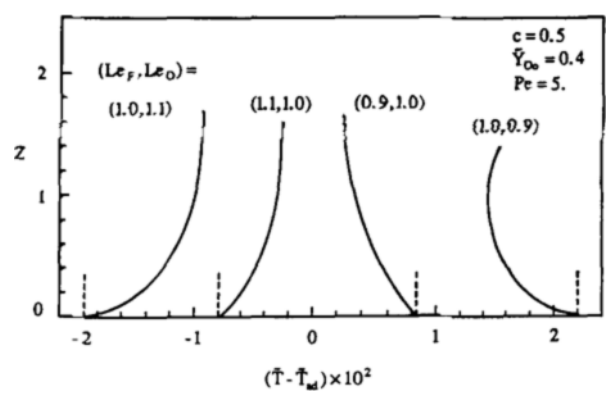

Fig. 4 Flame temperature along flame surface for small Pe (···; leading order, —— ; first order)

since mass diffusion of fuel is faster than thermal diffusion. It has the same effect of increasing fuel flow rate or fuel mass fraction at the nozzle exit. Conversely, Le_O has effect of decreasing flame length as it decreases.

Especially interesting effect of preferential diffusion is flame temperature variation along the flame, which could affect such phenomena as tip opening (Ishizuka, 1983), local blow-off, and local soot formation rate. The leading order solution of Eqs. (19) and (20) shows the uniform flame temperature while the first order solution would exhibit flame temperature variation. Figure 4 shows the flame temperature variation of an over-ventilated flame along the streamwise direction for small Peclet number and Fig. 5 is for large Peclet number. For $Le_F<1$, flame temperature de-

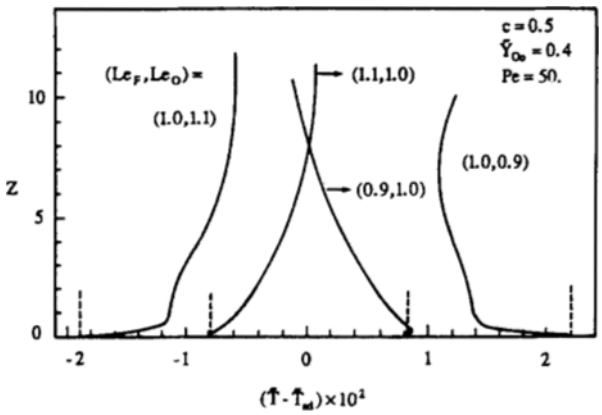

Fig. 5 Flame temperature along flame surface for largel Pe (···; leading order, —— ; first order)

creases in streamwise direction, having a minimum near the flame tip. This shows a possiblity of tip opening. For $Le_F > 1$, flame temperature is maximum at the tip, thus having a possibility of tip intensification.

Experimental results (Ishizuka, 1983) show that the flame temperature decreases along the streamwise direction and flame tip opening occurs for hydrogen with inerts of N_2, Ar, and CO_2. For hydrogen with He, on the other hand, the flame temperature increases. This is because hydrogen has faster mass diffusion velocity compared to N_2, Ar, and CO_2, thus $Le_F < 1$, while the velocity is comparable to He. the present results qualitatively agree with this.

Flame temperature characteristics for $Le_F \neq 1$ are similar to those of the two dimensional model (Chung and Law, 1984) except for $Le_o \neq 1$. Results for two dimensional case was qualitatively symmetric for $Le_o > 1$ and $Le_o < 1$. However for the present axisymmetric case, results show that for $Le_o > 1$, flame is intensified at the tip while for $Le_o < 1$, flame temperature has a minimum near the middle of the flame which indicated a possibility of local blowout. This can be attributed to the presence of two principal radii of curvatures compared to one for two dimensional case.

Flame temperature variation along the z axis by varying the Peclet numbers is shown in Figs. 6 and 7 for $Le_F \neq 1$ and $Le_o \neq 1$, respectively. For $Le_F \neq 1$, flame temperature distribution is quite similar near the rim region and it deviates significantly near the flame tip. For $Le_o \neq 1$, flame temperature distribution is quite different near the rim region and the tip temperatures are quite similar.

The reason for this can be explained as follows. If the direction of diffusion is parallel (opposed) to that of convection, convection diminishes (amplifies) the effect of preferential diffusion (Law and Chung, 1982). Near the base of the overventilated flame, the direction of oxidizer diffusion is parallel to that of the convection. Therefore, as the Peclet number increases, the convection would reduce the effect of nonunity Lewis number of oxidizer on flame temperature. Hence, the flame temperature approaches the adiabatic one. For fuel, however, since its direction of diffusion is opposite to that of convection, nonunity Lewis number effect of fuel is amplified.

In contrast, the direction of oxidizer diffusion is opposite to that of convection in the upper portion of the flame. Hence the flame temperature tends to deviate more from te adiabatic one as Pe increases. Since the two directions are

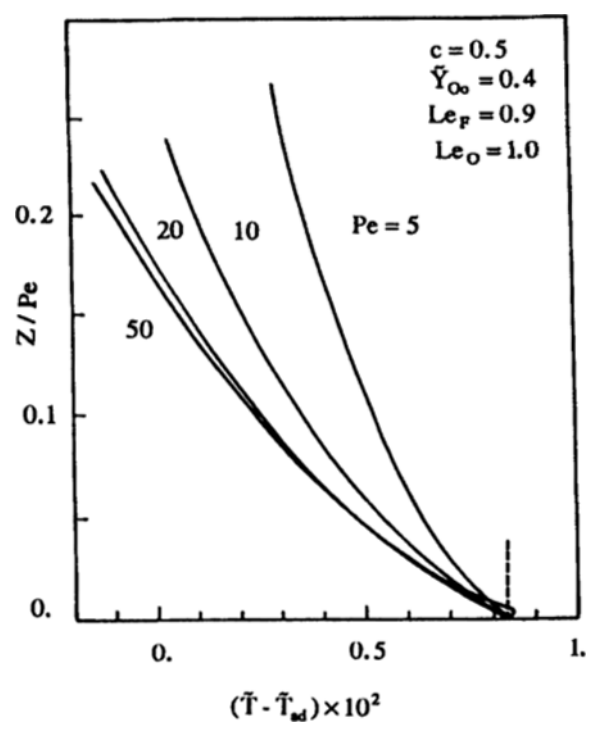

Fig. 6 Effect of Pe on flame temperature for $Le_F \neq 1$ (···; leading order, —— ; first order)

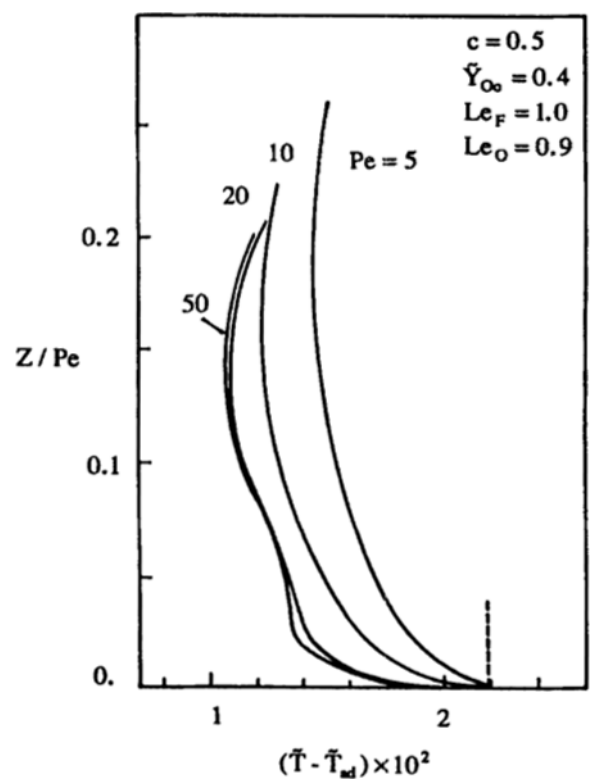

Fig. 7 Effect of Pe on flame temperature for $Le_o \neq 1$ (···; leading order, —— ; first order)

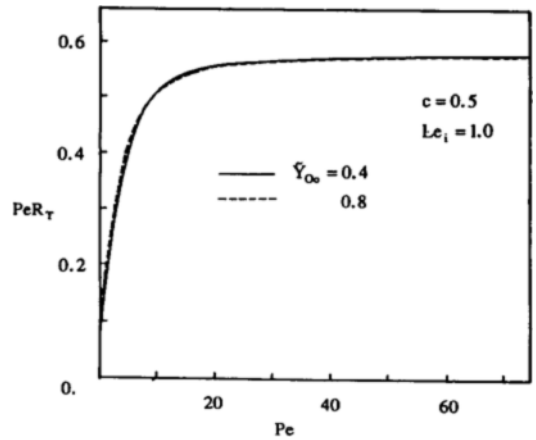

Fig. 8 Curvature at the flame tip as functions of Pe

parallel for fuel in this region, the flame temperature tends to approach the adiabatic one.

In two dimensional model with nonunity Le_F, effect of preferential diffusion diminishes as Pe increases since the directions of fuel mass diffusion and convection are parallel. Thereby, the temperature at the tip approaches the adiabatic one. However in the present cylindrical model, such an effect is not pronounced.

Experimental results of Ishizuka(1983) show that the tip opening occurs at a constant concentration and is independent of flow velocity except for very small convection velocities. Based on this, we have tested whether the tip opening is controlled by the flame stretch or not.

In a uniform flow field, a steady curved flame has a flame stretch proportional to v/R_T, where R_T is the radius of curvature(Matalon, 1983; Chung and Law, 1984b). At a constant concentration, the flame stretch v/R_T increases with the flow velocity since R_T decreases with v. This indicates that the flame stretch alone can not explain the tip opening phenomena properly.

By nondimensionalizing the stretch with a local characteristic flow time $(\lambda/\rho C_p)/v^2$, the nondimensional stretch becomes $(\lambda/\rho C_p)/vR_T = b/PeR_T$. Thus we have plotted PeR_T as a function of $\tilde{Y}_{oo}$ and Pe in Fig. 8. This shows that PeR_T is independent of v and also of $\tilde{Y}_{oo}$ for $Pe > 20$. Note here that $(\lambda/\rho C_p)$ is assumed constant in the present model.

In a realistic situations, $(\lambda/\rho C_p)$ is sensitive to $\tilde{Y}_{oo}$ through the flame temperature, thus PeR_T will vary with $\tilde{Y}_{oo}$. Therefore the tip opening condition of a constant concentration agrees with the constant nonimensional stretch of $(\lambda/\rho C_p)/vR_T$, meaning that the tip opening can be explained based on the nondimensional stretch.

5. CONCLUDING REMARKS

Effect of streamwise and preferential diffusion was analyzed for cylindrical B-S flame by using perturbation method with Le_i-1 as a small parameter. Results show that flame tip opening(intensification) could occur for $Le_F < 1 (> 1)$. Compared to the two dimensional problem, flame temperature behavior is not symmetric to the sign of $(Le_i - 1)$. This can be attributed to the geometrical factor of fuel defocusing and oxidizer focusing in mass diffusion. Finally, tip opening can be explained on the basis of the nondimensional stretch.

ACKNOWLEDGEMENT

This work was supported by the Agency for Defence Development under contract no. UD900072ED.

REFERENCES

Buckmaster, J.D. and Ludford, G.S.S., 1982, "Theory of Laminar Flames," Cambridge University Press.

Burke, S.P. and Schumann, T.E.W., 1928, "Diffusion Flames," Ind. Eng. Chem., Vol. 29, pp. 998~1004.

Chung, S.H. and Law, C.K., 1983, "Structure and Extinction of Convective Diffusion Flames with General Lewis Numbers," Combust. Flame, Vol. 52, pp. 59~79.

Chung, S.H. and Law, C.K., 1984a, "Burke-Schumann Flames with Streamwise and Preferential Diffusion," Combust. Sci. Tech., Vol. 37, pp. 21~46.

Chung, S.H. and Law, C.K., 1984b, "An Invariant Derivation of Flame Stretch," Combust. Flame, Vol. 55, pp. 123~125.

Chung, S.H. and Law, C.K., 1989, "Analysis of Some Nonlinear Premixed Flame Phenomena," Combust. Flame, Vol. 75, pp. 309~323.

Cohen, N.S., 1980, "Review of Composite Propellant Burn Rate Modeling," AIAA J., Vol. 18, pp. 277~293.

Glassman, I. and Yaccarino, P., 1981, "The Temperature Effect in Sooting Diffusion Flames," Eighteenth Symposium (International) on Combustion, The Combustion Institute, pp. 1175~1183.

Ishizuka, S., 1983, "An Experimental Study on the Opening of Laminar Diffusion Flame Tips," Nineteenth Symposium (International) on Combustion, The Combustion Institute, pp. 319~316.

Law, C.K. and Chung, S.H., 1982, "Steady State Diffusion Flame Structures with Lewis Number Variations," Combust. Sci. Tech., Vol. 29, pp. 129~145.

Law, C.K., Ishizuka, S. and Cho, P., 1982, "On the opening of Premixed Bunsen Flame TRips," Combust. Sci. Tech., Vol. 28, pp. 89~96.

Matalon, M., 1982, "On Flame Stretch," Combust. Sci. Tech., Vol. 31, pp 169~181.

Sivashinsky, G. I., 1983, "Instability, Pattern Formation, and Turbulence in Flames," Ann. Rev. Fluid Mech., Vol. 15, pp. 89~96.

Williams, F.A., 1985, "Combustion Theory," 2nd Ed., Benjamin/Cummings Publ. Co., Menro Park.

APPENDIX

· Green's Function Solutions of Eq.(17) and (18)

From Eq.(17) and (18), if we express

$$B_j(r,z) = \theta_j(r,z)\exp\left(\frac{Pe}{2}z\right) \tag{A1}$$

then θ_j becomes the solution of the Helmholtz equation of

$$\frac{Pe^2}{4}\theta_j - \nabla^2\theta_j = h_j \tag{A2}$$

where $h_j = 0$ in the leading order and $h_j = H_j\exp(-Pe\ z/2)$ in the first order. Boundary conditions are

$$N: \frac{\partial \theta_j}{\partial n}=0, \quad r=0,1 \tag{A3}$$

$$D: \theta_j=f, \quad z=0 \tag{A4}$$

$$\theta_j=0, \quad z\to\infty \tag{A5}$$

where N and D indicate Dirichlet and Neumann boundaries respectively, $\partial/\partial n$ the outward normal gradient, and f the transformed boundary condition with $f=0$ in the first order.

(1) Green's function formulation

The Green's function formulation of Eqs.(A2) ~ (A5) becomes

$$-\nabla^2 G(\boldsymbol{r}|\boldsymbol{r}_o)+k^2 G(\boldsymbol{r}|\boldsymbol{r}_o)=\delta(\boldsymbol{r}-\boldsymbol{r}_o) \tag{A6}$$

$$N: \frac{\partial G}{\partial n}=0 \tag{A7}$$

$$D: G=0 \tag{A8}$$

where $k=Pe/2$. From Eqs.(A2) and (A6)

$$\int_{V_r}\{G\nabla^2\theta_j-\theta_j\nabla^2 G\}dV_r=\int_{V_r}\{\theta_j\delta(\boldsymbol{r}-\boldsymbol{r}_o)-Gh_j\}dV_r \tag{A9}$$

Using Green's theorem, the LHS of Eq.(A9) becomes

$$\begin{aligned}\int_{V_r}\{G\nabla^2\theta_j-\theta_j\nabla^2 G\}dV_r&=\int_{\partial V_r}\left\{G\frac{\partial\theta_j}{\partial n_r}-\theta_j\frac{\partial G}{\partial n_r}\right\}dS_r\\&=\int_{D_r}\left\{G\frac{\partial\theta_j}{\partial n_r}-\theta_j\frac{\partial G}{\partial n_r}\right\}dS_r+\int_{N_r}\left\{G\frac{\partial\theta_j}{\partial n_r}-\theta_j\frac{\partial G}{\partial n_r}\right\}dS_r\\&=-\int_{\substack{D_r\\(z=0)}} f(\boldsymbol{r})\frac{\partial G}{\partial n_r}dS_r\end{aligned} \tag{A10}$$

and the RHS becomes

$$\int_{V_r}\{\theta_j\delta(\boldsymbol{r}-\boldsymbol{r}_o)-Gh_j\}dV_r=\theta_j(\boldsymbol{r}_o)-\int_{V_r}Gh_j dV_r \tag{A11}$$

From Eqs.(A10) and (A11)

$$\theta_j(\boldsymbol{r}_o)=\int_{V_r}G(\boldsymbol{r}|\boldsymbol{r}_o)\,h_j(\boldsymbol{r})\,dV_r-\int_{\substack{D\\(z=0)}} f(\boldsymbol{r})\,\frac{\partial G(\boldsymbol{r}|\boldsymbol{r}_o)}{\partial n_r}dS_r \tag{A12}$$

and from the symmetry of the Green's function

$$G(\boldsymbol{r}|\boldsymbol{r}_o)=G(\boldsymbol{r}_o|\boldsymbol{r}) \tag{A13}$$

$$\theta_j(\boldsymbol{r})=\int V_{r_o}G(\boldsymbol{r}|\boldsymbol{r}_o)\,h_j(\boldsymbol{r}_o)\,dV_{r_o}-\int_{\substack{D\\(z=0)}} f(\boldsymbol{r}_o)\,\frac{\partial G(\boldsymbol{r}|\boldsymbol{r}_o)}{\partial n_{r_o}}dS_{r_o} \tag{A14}$$

the problem reduces to finding a solution of Green's function of Eqs.(A6) ~ (A8)

(2) Green's function solution

The solution of the Green's function can be found from the eigenfunction expansion. If we expand $G(\boldsymbol{r}|\boldsymbol{r}_o)$ in Fourier-Bessel series

$$G(\boldsymbol{r}|\boldsymbol{r}_o)=g_0+\sum_{n=1}^{\infty}g_n(z)\,J_0(\lambda_n r) \tag{A15}$$

then from the orthogonality

$$g_0(z)=2\int_0^1 rG(\boldsymbol{r}|\boldsymbol{r}_o)\,dr \tag{A16}$$

$$g_n(z)=\frac{2}{J_0^2(\lambda_n)}\int_0^1 rG(\boldsymbol{r}|\boldsymbol{r}_o)\,J_0(\lambda_n r)\,ds, \quad n\geq 1$$

By substituting it to Eq.(A6), the transformed boundary value problem becomes

$$-\frac{d^2 g_o}{dz^2}+k^2 g_o=2r_o\delta(z-z_o) \tag{A17}$$

$$-\frac{d^2 g_n}{dz^2}+(k^2+\lambda_n^2)\,g_n=\frac{2r_o}{J_0^2(\lambda_n)}J_0(\lambda_n r_o)\,\delta(z-z_o), \quad n\geq 1 \tag{A18}$$

with the boundary conditions of

$$g_n(0)=0 \tag{A19}$$

$$g_n(\infty)=\text{bounded}, \quad n\geq 0$$

By substituting

$$g_n(z)=\frac{2r_o}{J_0^2(\lambda_n)}J_0(\lambda_n r_o)\,U_n(z) \tag{A20}$$

into Eq.(A18), it becomes

$$-\frac{d^2 U_n}{dz^2}+(k^2+\lambda_n^2)\,U_n=\delta(z-z_o) \tag{A21}$$

$$U_n(0)=0, \quad U_n(\infty)=\text{bounded}, \quad n\geq 0 \tag{A22}$$

The solution of Eqs.(A21) ~ (A22) is the same as that of the following O.D.E.

$$-\frac{d^2 U_n}{dz^2}+(k^2+\lambda_n^2)\,U_n=0, \quad 0\leq z<z_o, \; z_o\leq z\leq 1 \tag{A23}$$

$$U_n(0)=0, \quad U_n(\infty)=0 \tag{A24}$$

$$U_n(z_o^-)=U_n(z_o^+), \quad \left[-\frac{dU_n}{dz}\right]_{z_o^-}^{z_o^+}=1$$

and then the solution becomes

$$U_n=\frac{2}{\alpha_n}\begin{bmatrix}\exp\left(-\frac{\alpha_n}{2}z_o\right)\sinh\left(\frac{\alpha_n}{2}z\right), & z\leq z_o\\ \exp\left(-\frac{\alpha_n}{2}z\right)\sinh\left(\frac{\alpha_n}{2}z_o\right), & z\geq z_o\end{bmatrix} \tag{A25}$$

and the Green's function solution is

$$G(\boldsymbol{r}|\boldsymbol{r}_o)=\frac{4r_o}{Pe}\begin{bmatrix}\exp\left(-\frac{Pe}{2}z_o\right)\sinh\left(\frac{Pe}{2}z\right)\\ \exp\left(-\frac{Pe}{2}z\right)\sinh\left(\frac{Pe}{2}z_o\right)\end{bmatrix} \tag{A26}$$

$$+\sum_{n=1}^{\infty}\frac{4r_o J_0(\lambda_n r_o)}{\alpha_n J_0(\lambda_n)}J_0(\lambda_n r)\begin{bmatrix}\exp\left(-\frac{\alpha_n}{2}z_o\right)\sinh\left(\frac{\alpha_n}{2}z\right)\\ \exp\left(-\frac{\alpha_n}{2}z\right)\sinh\left(\frac{\alpha_n}{2}z_o\right)\end{bmatrix}\begin{matrix}z\leq z_o\\ z\geq z_o\end{matrix}$$

(3) Leading order solution

The leading order is homogeneous equation with $h_j=0$ from Eqs.(A2) and (A14) and since

$$\left|\frac{\partial G}{\partial n_r}\right|_{z=0}=-\left|\frac{\partial G}{dz}\right|_{z=o} \tag{A27}$$

the leading order solution becomes

$$\beta_j^0=\exp\left(\frac{Pe}{2}z\right)\int_0^1 F(r_o)\left\{\exp\left(-\frac{Pe}{2}z_o\right)\frac{\partial G}{\partial z}\right\}_{z_o=0}dr_o \tag{A28}$$

where $F(r_o)$ is the boundary condition at $z=0$. Hence from the boundary condition and Eq.(A25), it becomes

$$\beta_S^0=\left\{c^2\left(\frac{1}{Le_F}+\frac{\tilde{Y}_{Oo}}{Le_O}\right)-\frac{\tilde{Y}_{Oo}}{Le_O}\right\}+2c\left(\frac{1}{Le_F}+\frac{\tilde{Y}_{Oo}}{Le_O}\right)\sum_{n=1}^{\infty}\frac{J_1(\lambda_n c)}{\lambda_n J_0^2(\lambda_n)}J_0(\lambda_n r)\exp\left(\frac{Pe-\alpha_n}{2}z\right) \tag{A29}$$

$$\beta_T^0=\left(\frac{c^2}{Le_F}+\tilde{T}_o\right)+\frac{2c}{Le_F}\sum_{n=1}^{\infty}\frac{J_1(\lambda_n c)}{\lambda_n J_0^2(\lambda_n)}J_0(\lambda_n r)\exp\left(\frac{Pe-\alpha_n}{2}z\right) \tag{A30}$$

(4) First order solution

Th first order equation has homogeneous boundary conditions such that $f(\boldsymbol{r}_o)=0$ from Eq.(A14). Thus

$$\beta_j^1=\exp\left(\frac{Pe}{2}z\right)\int_{V_{r_o}}G(\boldsymbol{r}|\boldsymbol{r}_o)H_j(\boldsymbol{r}_o)\exp\left(-\frac{Pe}{2}z_o\right)dV_{r_o} \tag{A31}$$

where

$$H_T=-Pe\frac{\partial\tilde{Y}_F^0}{\partial z},\quad H_S=-Pe\frac{\partial}{\partial z}\left[\tilde{Y}_F^0+\frac{1_O}{1_F}\tilde{Y}_O^0\right]$$

with

$$\frac{\partial\tilde{Y}_F^0}{dz}=\left[\frac{\partial\beta_S^0}{\partial z}\right]_{\text{fuel side}},\quad\frac{\partial\tilde{Y}_O^0}{\partial z}=-\left[\frac{\partial\beta_S^0}{\partial z}\right]_{\text{oxi.side}}$$

Therefore the first order solution becomes

$$\beta_T^1=\exp\left(\frac{Pe}{2}z\right)\int_{V_F}\left\{g_0+2\sum_{n=1}^{\infty}\frac{r_o}{J_0^2(\lambda_n)}J_0(\lambda_n r_o)J_0(\lambda_n r)\,U_n\right\}\times\left\{-Pe\sum_{m=1}^{\infty}\phi_m J_0(\lambda_m r_o)\exp\left(\frac{Pe-\alpha_m}{2}z_o\right)\right\}\exp\left(-\frac{Pe}{2}z_o\right)dV_{r_o} \tag{A32}$$

$$\beta_S^1=\beta_T^1+\exp\left(\frac{Pe}{2}z\right)\left(\frac{Le_O-1}{Le_F-1}\right)\int_{V_O}\left\{g_0+2\sum_{n=1}^{\infty}\frac{r_o}{J_0^2(\lambda_n)}J_0(\lambda_n r_o)J_0(\lambda_n r)\,U_n\right\}\times\left\{-Pe\sum_{m=1}^{\infty}\phi_m J_0(\lambda_m r_o)\exp\left(\frac{Pe-\alpha_m}{2}z_o\right)\right\}\exp\left(-\frac{Pe}{2}z_o\right)dV_{r_o} \tag{A33}$$

where

$$\phi_n=c(1+\nu)J_1(\lambda_n c)(Pe-\alpha_n)/\{\lambda_n J_0^2(\lambda_n)\} \tag{A34}$$

and F and O indicates the fuel and oxidizer side respectively in the leading order flame sheet limit. The above equations have the following double integrals for r_o and z_o.

(a) Overventilated case

The double integral are as follows

$$\int_{V_F}(.)\,dV_{r_o}=\int_0^{z_f}\int_0^{r_f^o}(.)\,dr_o dz_o \tag{A35}$$

$$\int_{V_O}(.)\,dV_{r_o}=\int_0^{z_f}\int_{r_f^o}^{1}(.)\,dr_o dz_o+\int_{z_f}^{\infty}\int_0^1(.)\,dr_o z_o \tag{A36}$$

where $r_f^o(z_o)$ is the flame location in the leading order for a given z_o, and Z_f is the leading order flame height.

The first order solution from Eqs.(A32) and (A33) are as follows.

$$\beta_S^1=\left(1-\frac{Le_O-1}{Le_F-1}\right)\beta_T^1-\frac{Le_O-1}{Le_F-1}zPe\sum_{n=1}^{\infty}\phi_n J_0(\lambda_n r)\exp\left(\frac{Pe-\alpha_n}{2}z\right)/\alpha_n \tag{A37}$$

$$\beta_T^1=-2Pe\exp\left(\frac{Pe}{2}z\right)\left[\sum_{m=1}^{\infty}\int_0^{Z_f}\phi_m U_o\exp\left(-\frac{\alpha_m}{2}z_o\right)\frac{r_f^o J_1(\lambda_m r_f^o)}{\lambda_m}dz_o+\sum_{n=1}^{\infty}\frac{J_0(\lambda_n r)}{J_0^2(\lambda_n)}\int_0^{Z_f}U_n\phi_n\exp\left(-\frac{\alpha_n}{2}z_o\right)\frac{r_f^{o2}}{2}\{J_1^2(\lambda_n r_f^o)+J_0^2(\lambda_n r_f^o)\}dz_o+\sum_{n=1}^{\infty}\frac{J_0(\lambda_n r)}{J_0^2(\lambda_n)}\int_0^{Z_f}U_n\sum_{\substack{m=1\\m\neq n}}^{\infty}\phi_m\exp\left(-\frac{\alpha_m}{2}z_o\right)\frac{r_f^{o2}}{\lambda_m^2-\lambda_n^2}\times\{\lambda_m J_0(\lambda_n r_f^o)J_1(\lambda_m r_f^o)-\lambda_n J_0(\lambda_m r_f^o)J_1(\lambda_n r_f^o)\}dz_o\right]\equiv\Gamma \tag{A38}$$

(b) Under-ventilated case

The double integrals are

$$\int_{V_O}(.)\,dV_{r_o}=\int_0^{z_f}\int_{r_f^o}^{1}(.)\,dr_o dz_o \tag{A39}$$

$$\int_{V_F}(.)\,dV_{r_o}=\int_0^{z_f}\int_0^{r_f^o}(.)\,dr_o dz_o+\int_{z_f}^{\infty}\int_0^1(.)\,dr_o dz_o \tag{A40}$$

which has same β_S^1 as Eq.(A37), and β_T^1 is

$$\beta_T^1=\Gamma-Pe\exp\left(\frac{Pe}{2}z\right)\sum_{n=1}^{\infty}J_0(\lambda_n r)\,\delta_n/2 \tag{A41}$$

where

$$\delta_n=2\phi_n\begin{cases}2\exp(-\alpha_n Z_f)\sinh(\alpha_n z/2)/\alpha_n^2, & z\le Z_f\\ \exp(-\alpha_n z/2)[(z+1/\alpha_n)-\{Z_f+\exp(-\alpha_n Z_f)/\alpha_n\}]/\alpha_n, & z\ge Z_f\end{cases}$$